

University of Wollongong Research Online

Faculty of Engineering - Papers (Archive)

Faculty of Engineering and Information
Sciences

1-1-2010

The behavior of precipitates during hot-deformation of low-manganese, titanium-added pipeline steels

Ali Dehghan-Manshadi
University of Wollongong, alidm@uow.edu.au

Rian J. Dippenaar
University of Wollongong, rian@uow.edu.au

Follow this and additional works at: <https://ro.uow.edu.au/engpapers>



Part of the [Engineering Commons](#)

<https://ro.uow.edu.au/engpapers/988>

Recommended Citation

Dehghan-Manshadi, Ali and Dippenaar, Rian J.: The behavior of precipitates during hot-deformation of low-manganese, titanium-added pipeline steels 2010, 3291-3296.
<https://ro.uow.edu.au/engpapers/988>

Research Online is the open access institutional repository for the University of Wollongong. For further information contact the UOW Library: research-pubs@uow.edu.au

The Behavior of Precipitates during Hot-Deformation of Low-Manganese, Titanium-Added Pipeline Steels

ALI DEGHAN-MANSHADI and RIAN J. DIPPENAAR

The behavior of manganese and titanium sulfides during the hot deformation of a low-carbon, low-manganese, titanium-added steel has been studied using transmission electron microscopy (TEM), scanning electron microscopy (SEM), and energy-dispersive spectrometry (EDS) analysis. In addition, the effects of deformation temperature and strain rate on the size and distribution of precipitates have been studied using an automatic inclusion analysis system. Also, the effect of precipitate distribution on mechanical properties was studied at different deformation conditions of temperature and strain rate. The TEM and SEM analyses revealed the presence of a wide variety of simple and/or complex precipitates in the as-cast structure. These precipitates behaved differently during the hot deformation of steel. Precipitates deformed less at higher deformation temperatures, whereas an increase in strain rate increased the elongation of precipitates.

DOI: 10.1007/s11661-010-0515-9

© The Minerals, Metals & Materials Society and ASM International 2010

I. INTRODUCTION

IT is well documented that the formation and segregation of a variety of precipitates during continuous casting have significant effects on microstructural development and, consequently, on the mechanical properties of the steel product during and after hot rolling.^[1,2] Manganese, in particular, is of great significance because MnS precipitates deform plastically along the rolling direction, resulting in poor toughness in the material.^[3,4] During solidification, manganese tends to segregate toward the centerline, and large manganese sulfides form in this region. Therefore, if the segregation of manganese can be reduced, then it follows that the formation of MnS precipitates in the centerline regions will also be reduced. To achieve such a goal, it is vitally important to improve the understanding the mechanism and rate of MnS precipitation during solidification, however, importantly, the behavior of these precipitates during hot rolling.

Several attempts, including improved casting conditions as well as appropriate adjustments to the chemical composition of steel, for instance the addition of microalloying elements such as titanium, niobium, and chromium,^[5-7] have been made to reduce centerline segregation of precipitates in continuously cast slabs. Many attempts have been made in the past to encourage the formation of small, preferably spherically shaped and evenly distributed precipitates across the slab in a homogeneous manner.

Despite progress toward encouraging more uniform distribution of precipitates and to reduce the number of large sulfide precipitates forming at the centerline, industrially produced steel slabs still contain these large precipitates in segregated areas.^[8] The most common and obvious strategy to reduce the precipitation of sulfide inclusions at the centerline of steel slabs is to reduce the sulfur content of the steel. However, desulfurization is costly and time consuming, adding significantly to production cost. An alternative approach to the reduction of manganese sulfide precipitation at the centerline is to decrease the manganese content of the steel, which is usually in the range of 1.0 to 1.5 in the high-strength pipeline steels^[9,10] to about 0.3 pct. The important contribution of manganese to solid solution strengthening can be then compensated for by the addition of small amounts of alloying elements, such as Ti, Cr, and Nb. Such elements can also combine with manganese and sulfur to form sulfides that are harder than MnS. Therefore, those precipitates will deform less plastically during deformation of steel. The new precipitates can still prevent the hot shortness (*i.e.*, formation of FeS). The sulfides of these alloying elements are usually smaller than MnS precipitates and do not elongate during hot rolling. Hence, the toughness of the proposed low-manganese steels should not be affected adversely compared with high-manganese steels, especially not in the transverse direction.

Although centerline precipitation in low-manganese steels has been reduced significantly,^[10] there remains some degree of manganese segregation, and hence MnS precipitation in these regions. This observation emphasizes the importance of gaining an improved understanding of the behavior of these precipitates during hot rolling of the newly developed low-manganese steels. In the current investigation, deformation of different centerline precipitates was studied under different deformation conditions using hot-compression tests of a

ALI DEGHAN-MANSHADI, Research Fellow, and RIAN J. DIPPENAAR, Professor, are with the Faculty of Engineering, University of Wollongong, Wollongong 2500, NSW, Australia. Contact e-mail: alidm@uow.edu.au

Manuscript submitted July 7, 2010.

Article published online October 28, 2010

low-manganese, titanium-added pipeline steel. Also, the effect of such precipitates on the deformation behavior of the steel and on the resulting mechanical properties was assessed.

II. EXPERIMENTS

A low-carbon, low-manganese steel containing 0.075 pct C, 0.3 pct Mn, 0.019 pct S, 0.011 pct P, and 0.026 pct Ti has been used for the purposes of studying the behavior of manganese sulfide precipitates during deformation. Plane-strain compression specimens with dimensions of $20 \times 15 \times 10$ mm were cut from the centerline of as-cast slabs supplied by BlueScope Steel Ltd, Australia. Hot-compression tests were carried out in a Gleeble 3500 thermomechanical simulator (Dynamic Systems Inc., Poestenkill, NY). Samples were heated to 1373 K (1100 °C) at a rate of 5 K s^{-1} and held for 300 s, aiming to obtain a homogenized microstructure. The samples were then cooled to different temperatures and deformed at two different strain rates, 1 s^{-1} and 10 s^{-1} , respectively, to a strain of 1.2, followed by a rapid water quench (Figure 1).

The particular geometry of plane-strain compression samples in the Gleeble thermomechanical simulator provides the unique opportunity to study deformed and undeformed areas in a single specimen, subjected to the exact same thermal treatment save for the deformation (Figure 1). This feature enabled a study of the behavior of precipitates during hot deformation by a direct comparison of the deformed and undeformed areas under different conditions of reheating and deformation.

Field-emission gun scanning electron microscopy (FEG-SEM) studies were carried out using a JEOL JSM-7001F thermal field emission instrument (Jeol, Tokyo, Japan) to quantify the morphology and composition of sulfide precipitates. Transmission electron microscopy (TEM) was also used to characterize small particles, mostly of titanium nitride. The distribution of precipitates was studied using an automatic inclusion

analyzing system (Bruker-Quantax 400 Steel) attached to the FEG-SEM. In this system, all precipitates in a large surface of polished sample can be identified (by image processing), analyzed (using X-ray spectrometry), and classified (using special software called “Esprit steel”).

III. RESULTS AND DISCUSSION

Prior to studying the deformation behavior of precipitates and their effect on mechanical properties, TEM, SEM, and automatic inclusion analysis were conducted on specimens extracted from the centerline of as-cast slabs to characterize the nature, morphology, and distribution of centerline precipitates. This study revealed the presence of a large number of different kinds of precipitate with several different morphologies as shown in Figure 2. The precipitates usually had a large spread in chemical composition, size, and shape, as well as constituent phases. Most of the precipitates were identified as small or large stringers of MnS or TiS, being the most common precipitates normally present in continuously cast steels containing manganese, titanium, and sulfur. The small and the large particles of MnS were all concentrated around the centerline of the slab (Figure 2). They were usually circular or semicircular in shape with some being elongated, as shown in Figure 2(b).

Ti-sulfide and/or carbosulfides were observed frequently in the microstructures. Usually, these precipitates were observed as small circularly shaped particles (Figure 2(b)). However, in several cases, both MnS and TiS were detected in different parts of a single precipitate as two different constituent phases (Figures 2(c) and (d)). It seems that one phase has formed during the earlier stages of solidification (or cooling) and acted as nucleation sites for the second phase. Because of the limitation in accuracy of EDS analyses, it is neither possible to distinguish between sulfide and carbosulfides nor to determine the exact composition of the precipitates in the steel. Yoshinaga *et al.*^[11] proposed that TiS can be distinguished from $\text{Ti}_4\text{C}_2\text{S}_2$ because $\text{Ti}_4\text{C}_2\text{S}_2$ precipitates have a Ti/S peak ratio of almost 2. The EDS analyses using both TEM and SEM in the current study have shown that most of the Ti- and S-containing precipitates had a Ti/S ratio very close to 2; therefore, these particles are most likely to be $\text{Ti}_4\text{C}_2\text{S}_2$, rather than TiS. Iorio and Garrison^[12] have shown that the formation of $\text{Ti}_4\text{C}_2\text{S}_2$ precipitates is more probable than the formation of TiS in steel with carbon content higher than 0.02 pct, such as the steel under investigation. However, an accurate TEM analysis of a similar steel by Aminorroaya and Dippennar^[13] has shown clearly the formation of FeTiS_2 as another possible precipitate. They then argued that these FeTiS_2 precipitates can act as nucleation sites for MnS precipitation.

EDS analyses of some precipitates in this work revealed the presence of manganese, titanium, and sulfur in a single precipitate, indicating the possible formation of $[\text{Ti} + \text{Mn}]S$ precipitates. However, it should be borne in mind that $[\text{Ti} + \text{Mn}]S$ precipitates

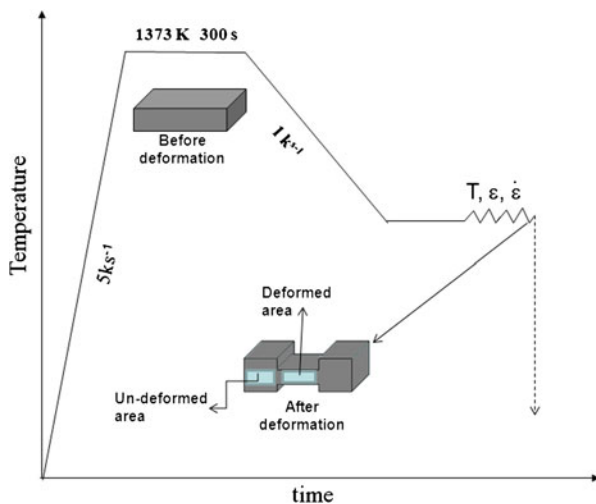


Fig. 1—Schematic diagram of hot deformation schedule and sample geometry before and after deformation.

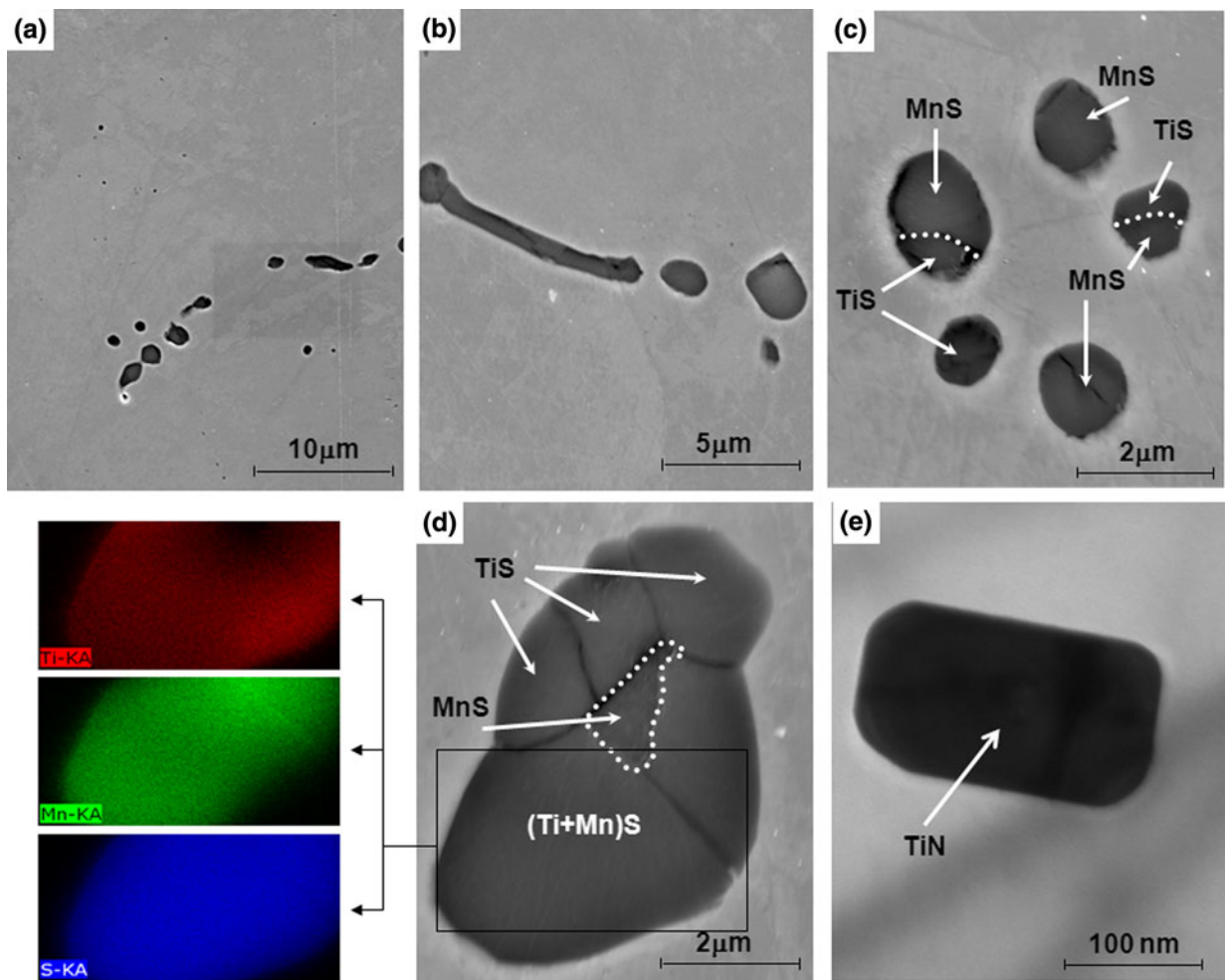


Fig. 2—Electron micrographs of different precipitate types and shapes at the centerline of an as-cast steel.

are not likely to form in steel because of the structural differences between manganese and titanium sulfides. However, the EDS data shown in Figure 2(d) indicate the presence of both titanium and manganese in a single sulfide precipitate, and it is, therefore, important that the exact nature and structure of such precipitate be analyzed in more detail using more advanced analytical techniques, such as atom probe analysis.

Titanium nitride (TiN) precipitates were observed frequently as small, cuboid-shaped precipitates in the TEM images (Figure 2(e)). This observation is not surprising because the presence of TiN precipitates is common in titanium-containing steels, and they are the most stable precipitates at high temperature.^[14]

In some large precipitates, manganese-enriched precipitates were surrounded by Ti-enriched precipitates, as shown in Figure 3. This observation can be explained if it is assumed that MnS nucleated during the early stages of solidification/cooling, then titanium atoms were rejected from the MnS growth front during the growth of the precipitate. When the titanium concentration reached a critical value during cooling, titanium sulfide or carbosulfide then formed as a shell around the MnS particle.

By using the automatic inclusion analysis system attached to the FEG-SEM, it was found that a wide range of particles with different sizes and size distributions precipitated at the centerline of the as-cast slabs as shown in Figure 4. It is evident that a large fraction of precipitates are of circular (or near circular) shape with aspect ratios varying between 1 and 3, and some precipitates exist with aspect ratios larger than 10. Metallographic observations showed that these precipitates are usually rod-shaped MnS particles, as previously shown in Figure 2(b). The relative frequency of precipitate length, which is superimposed in Figure 4, indicates that more than 90 pct of precipitates have a length between 1 and 4 μm, with only a few of them longer than 8 μm. Earlier research has shown that precipitates larger than 1 μm can elongate during hot deformation^[15] and that the extent of elongation is a function of precipitate size (at least for precipitates ranging from 1 to 5 μm^[3]), it is expected that these precipitates will elongate along the direction of deformation and, hence, will affect the mechanical properties of the deformed steel.

To understand fully the effect of centerline precipitates and the way in which they deform, on the

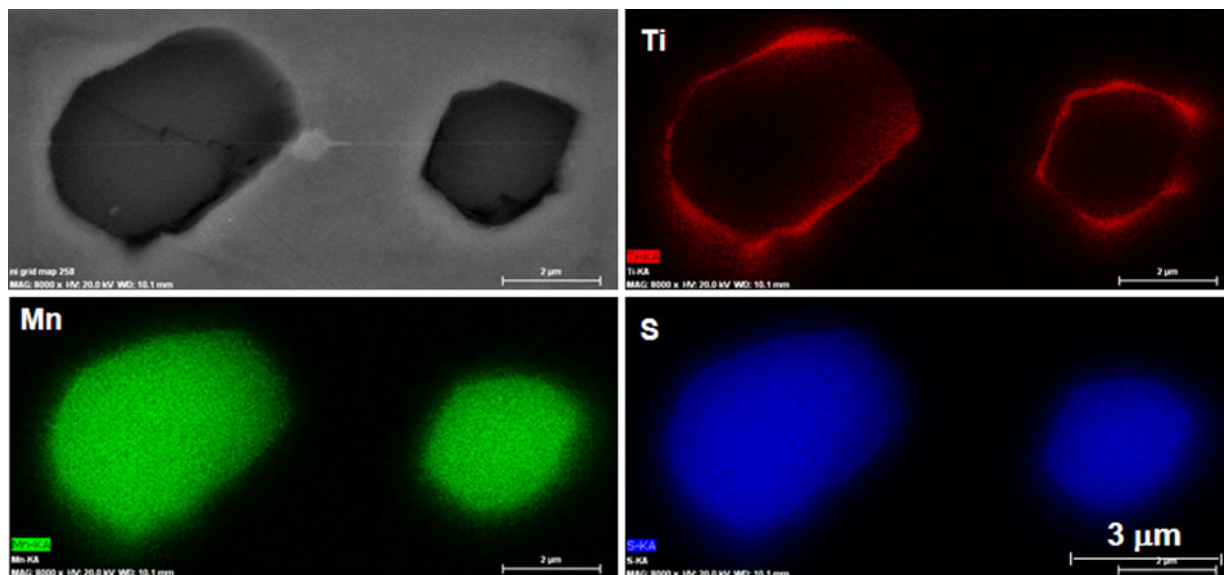


Fig. 3—EDS analyzing of precipitates showing presence of TiS around MnS precipitates.

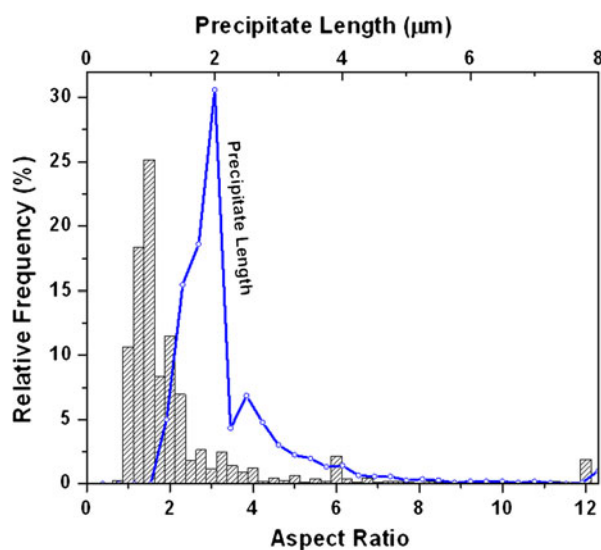


Fig. 4—Relative frequency for aspect ratio and length of centerline precipitates in as-cast steel.

mechanical properties of low-manganese steel, flow curves were determined in Gleeble tests under different deformation conditions and subsequently analyzed. Figure 5 shows examples of typical flow curves for specimens deformed at different temperatures and strain rates. Under all conditions, the flow stress increased with increasing strain to a peak value followed by a gradual fall toward a steady state, strongly suggesting that dynamic recrystallization (DRX) of austenite is occurring in the course of the test. However, there are significant differences in the shapes of the flow curves after deformation at different strain rates, which means that restoration mechanisms other than dynamic recrystallization might be operating under certain conditions of deformation. For example, the peak-stress becomes less prevalent as the temperature of deformation is

lowered and is completely absent at a deformation temperature of 1173 K (900 °C) and a strain rate of 10 s^{-1} . The disappearance of a peak in the flow curve suggests that the kinetics of DRX is slow under these conditions, and therefore, other mechanisms are responsible for restoration during hot deformation. Moreover, the specific shape of the flow curves (*i.e.*, increasing stress to a maximum and then maintaining a steady state) for samples deformed at 1273 K (1000 °C) and 10 s^{-1} , indicates that dynamic recovery (DRV) could be the responsible restoration mechanism.^[16] It is likely that different responses of precipitates to varying deformation conditions can influence the shape of the flow curves, and it was important to examine in detail such a possibility by analyzing the behavior of precipitates during deformation by the use of automatic inclusion analyses.

To study the behavior of precipitates during hot deformation, the morphology (aspect ratio) and size of precipitates were studied on deformed areas of Gleeble samples and compared with undeformed areas and the as-cast samples. As manganese sulfides are considered highly deformable precipitates, this comparison should show a clear effect of deformation on the elongation of precipitates. Figure 6 shows the effect of deformation on the aspect ratio of specimens deformed at 1273 K (1000 °C) at a strain rate of 1 s^{-1} . It is clear that the aspect ratio of precipitates is increased by deformation of the steel samples and that this increase in the aspect ratio also increases with the size of the precipitates. It is generally accepted that precipitates smaller than $1 \mu\text{m}$ are essentially not deformable,^[15] but it is clear from Figure 6 that the deformability of larger precipitates depends on their size. The diversion between two ellipses in Figure 6 indicates more increase in the aspect ratio of larger precipitates. Figure 6 also shows that some precipitates in undeformed samples have large aspect ratios. It is most likely that these are preexisting rod-like precipitates such as those shown in Figure 2(b).

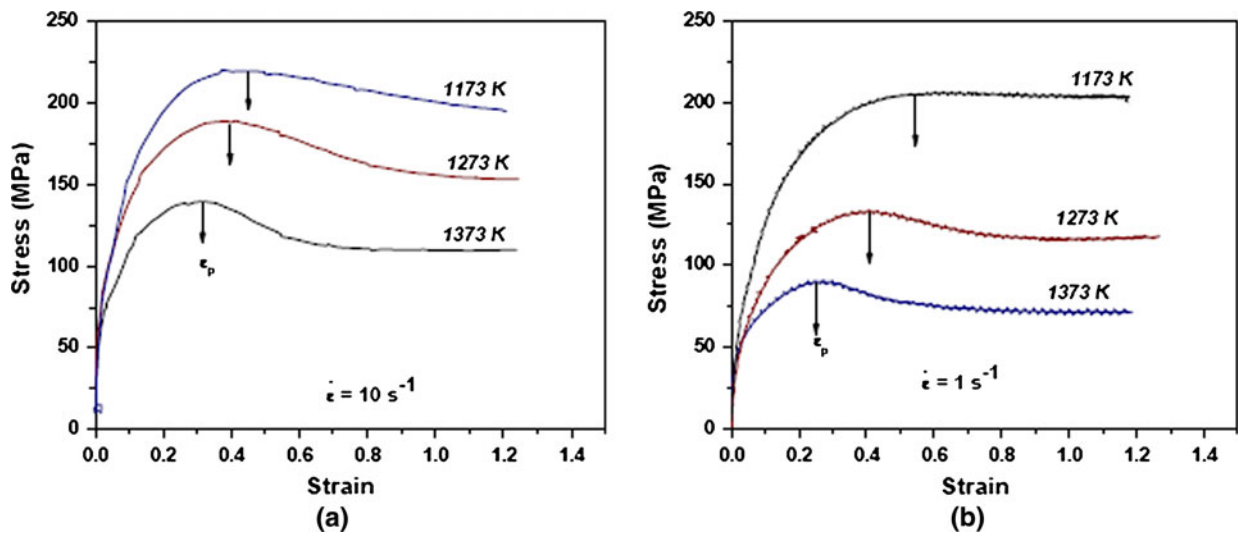


Fig. 5—Flow curves of centerline samples deformed at different deformation conditions.

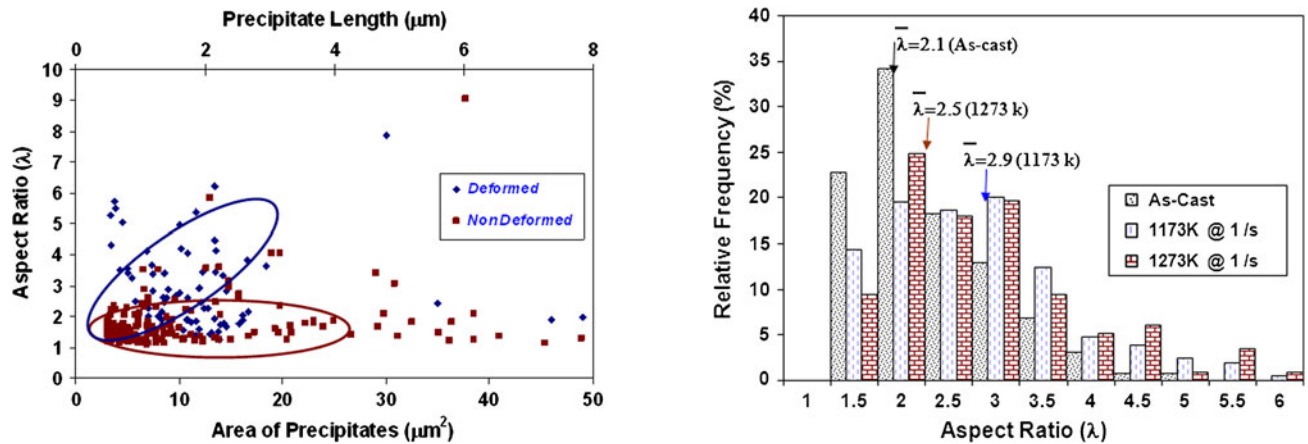


Fig. 6—A comparison between the aspect ratios of precipitates in deformed (at 1273 K (1000 °C)) and nondeformed areas of Gleeble samples.

However, such large precipitates were not observed in deformed samples, which could be attributed to the fact that the large and rod-like precipitates break down to the smaller precipitates during deformation.

It is to be expected that the deformation temperature will affect the extent to which precipitates will elongate. Luo and Stahlberg^[17] have confirmed that an increase in the deformation temperature from 1173 K (900 °C) to 1473 K (1200 °C) leads to a decrease in the extent of deformation of MnS precipitates in steel. In the current study, the influence of the temperature of deformation on the deformation behavior of precipitates was explored extensively by analyzing the precipitate size after deformation at 1173 K and 1273 K ((900 °C and 1000 °C), respectively). These results, which are shown in Figure 7, indicate that the precipitates in samples deformed at 1273 K (1000 °C) are less elongated and have a smaller average aspect ratio than precipitates in samples deformed at 1173 K (900 °C). The fact that MnS precipitates deformed less at a higher temperature

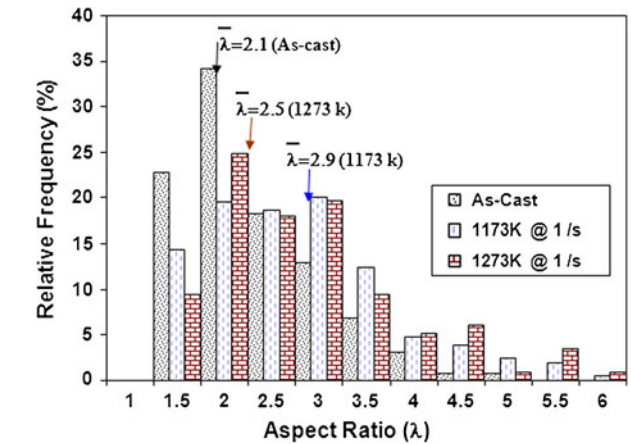


Fig. 7—Relative frequency for aspect ratio of precipitates deformed at different temperatures ($\bar{\lambda}$ in each group is the mean value of at least 300 precipitates).

might be attributed to the relative difference in hardness of the steel matrix and the precipitates. This consideration implies that recrystallization, recovery, and strain hardening of austenite need to be considered, as these restoration processes will have a determining influence on the hardness of the austenite relative to that of the precipitates. Vodopivec and Gabrovsek^[3] argued that at a lower deformation temperature, the volume fraction of dynamically recrystallized austenite will be lower; therefore, the austenite will be harder. Hence, at lower deformation temperatures, the ratio of austenite hardness to precipitate hardness is increased. Consequently, the relative plasticity of MnS precipitates is increased, and they will elongate more as shown in Figure 7. To explore the validity of this argument, the deformation of precipitates were examined under different strain rates at the same temperature. As shown previously (Figure 5), DRX kinetics decrease with increasing strain rate; hence, the austenite should be relatively harder at higher strain rates, and precipitates should deform more at

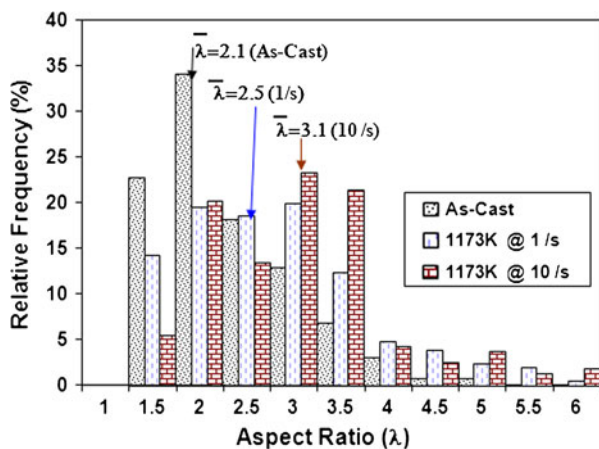


Fig. 8—Relative frequency for aspect ratio of precipitates deformed at different strain rates ($\bar{\lambda}$ in each group is the mean value of at least 300 precipitates).

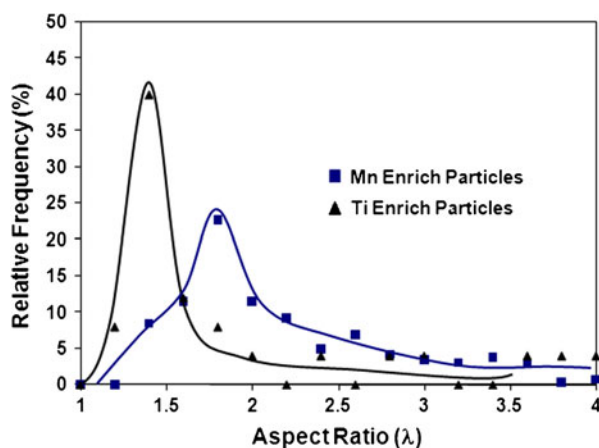


Fig. 9—A comparison between the relative frequency of Mn-enriched and Ti-enriched precipitates after deformation at 1173 K (900 °C) and a strain rate of 10 s^{-1} .

higher strain rates. A histogram of the aspect ratio of precipitates deformed at strain rates of 1 and 10 s^{-1} , shown in Figure 8, provides evidence of the validity of this argument because precipitates in samples deformed at 10 s^{-1} were elongated more than those in samples deformed at a strain rate of 1 s^{-1} . The difference in behavior of precipitates in samples subjected to different strain rates can also explain the differences in the shapes of the flow curve of samples deformed under different strain rates.

Figure 9 compares the deformation of Mn-enriched and Ti-enriched precipitates, and it is evident that the deformation behavior of precipitates is a function of their chemical composition. Ti-enriched precipitates are stronger than their Mn-enriched counterparts and deform less during the hot deformation of steel. However, it is important to note that the Ti-enriched precipitates (i.e., Ti sulfide or carbosulfides) in as-cast

structure are always smaller than the MnS precipitates. Therefore, the fact that Ti-enriched precipitates elongated less than MnS precipitates could possibly be attributed to their smaller size. However, Ti-enriched precipitates are always harder than Mn-enriched precipitates and are more difficult to elongate during deformation.^[4]

IV. CONCLUSIONS

A study on deformation behavior of different precipitates in an as-cast low-C, low-Mn, Ti-added steel revealed a considerable effect of precipitates elongation on mechanical properties of steel at the end of deformation process. The results showed that the elongation of MnS precipitates increased by decreasing deformation temperature or by increasing strain rate. Also, the investigations showed more elongation of Mn-enriched precipitates compared with Ti-enriched precipitates.

ACKNOWLEDGMENTS

This work was conducted as part of an ARC-Linkage Grant LP0669602 with BlueScope Steel as Industrial Partner. We gratefully acknowledge the financial support of the ARC and Bluescope Steel. We also wish to thank the University of Wollongong for the provision of laboratory facilities and the encouragement to conduct this investigation.

REFERENCES

1. G. Krauss: *Metall. Mater. Trans. B*, 2003, vol. 34B, pp. 781–92.
2. Y. Ito, N. Masumitsu, and K. Matsubara: *ISIJ Int.*, 1981, vol. 21, pp. 477–84.
3. F. Vodopivec and M. Gabrovsek: *Met. Technol.*, 1980, vol. 7, pp. 186–91.
4. R. Kiessling and N. Lange: *Non-Metallic Inclusions in Steel*, 2nd ed., The Institute of Materials, London, UK, 1997.
5. H. Kejian and T.N. Baker: *Mater. Sci. Eng.*, 1993, vol. A169, pp. 53–65.
6. M. Charleux, W.J. Poole, M. Militzer, and A. Deschamps: *Metall. Mater. Trans. A*, 2001, vol. 32A, pp. 1635–47.
7. K. Oikawa, K. Ishida, and T. Nishizawa: *ISIJ Inter.*, 1997, vol. 37, pp. 332–38.
8. L. Zhang and B. Thomas: *Metall. Mater. Trans. B*, 2006, vol. 37B, pp. 733–61.
9. J.M. Gray: U.S. Patent 5 993 570, 1999.
10. J.G. Williams: *3rd Int. Conf. TMP*, Associazione Italiana Di Metallurgia, 2008.
11. N. Yoshinaga, K. Ushioda, S. Akamatsu, and O. Akisue: *ISIJ Int.*, 1994, vol. 34, pp. 24–32.
12. L.E. Iorio and W.M. Garrison: *ISIJ Int.*, 2002, vol. 42, pp. 545–50.
13. S. Aminorroaya and R. Dippennar: *J. Microsc.*, 2007, vol. 227, pp. 92–97.
14. S.F. Medina, M. Chapa, P. Valles, A. Qusipe, and M.I. Vega: *ISIJ Int.*, 1999, vol. 39, pp. 930–36.
15. A. Segal and J.A. Charles: *Met. Technol.*, 1977, vol. 4, pp. 177–82.
16. A. Dehghan-Manshadi, M.R. Barnett, and P.D. Hodgson: *Mater. Sci. Eng. A*, 2008, vol. 458, pp. 664–72.
17. C. Luo and U. Stahlberg: *Scand. J. Metall.*, 2002, vol. 31, pp. 184–90.